Simulating the Fuel Recipe in a Sodium-cooled Fast Reactor

Louis Kissinger

August 9, 2017

Abstract

Fuel cycle analysis is necessary to predict and prepare for many of the challenges in the near and distant future of nuclear engineering. Rigorous analysis of proposed fuel cycles is a prerequisite for application of advanced reactor design and long-term waste storage, both of which will determine the energy supply of the United States as fossil fuels are exhausted and humans move to a sustainable source of energy. This report is an investigation of the isotopic compositions of fresh and spent fuel in a 1000-MWth Metallic-Fuel Sodium Fast Reactor (SFR). The investigation used Serpent2, a Monte-Carlo based reactor simulation software, to simulate the operation of an SFR for 365 days. The findings were recorded in an XML database for use in the Cycamore reactor model in the CYCLUS framework. CYCLUS is an agent-based fuel cycle simulator that will use the results of this investigation to evaluate the effects of various decisions regarding the fuel cycle at various scales. The fresh fuel of this reactor is composed of 21 nuclides, including isotopes of Uranium, Neptunium, Plutonium, Americium, and Curium. The spent fuel of the reactor contains over a thousand different nuclides. All of the results of this investigation have been uploaded to a private repository on GitHub, including an XML database detailing the fresh and spent compositions of the fuel.

1. Introduction

1.1 Problem Statement and Motivation

Nearly every nation on Earth, including the United States, is dependent primarily on fossil fuels as an energy supply. This practice is the leading cause of global climate change, which threatens to end life on Earth. The most realistic solution to this issue is to develop a sustainable energy supply based on clean fuels with no greenhouse gas emissions. It is clear that this goal is impossible without significant advances in nuclear power technology. It is therefore necessary to rigorously analyze the fuel cycle in order to facilitate a transition to an energy economy based on advanced nuclear power.

The Department of Energy has proposed many transition plans to upgrade the US's fleet of nuclear reactors from the thermal light water reactors of today to advanced reactors with more sophisticated fuel compositions and cooling, reflecting, and moderating mechanisms. CYCLUS is well-equipped to solve problems of this scale, so all data recorded by this research will be saved to a private GitHub repository which members of the Advanced Reactor and Fuel Cycle (ARFC) research group at University of Illinois at Urbana-Champaign (UIUC) may access. ARFC researchers will use the findings of this investigation to prepare simulations in CYCLUS under the Cycamore model.

Additionally, the results of this investigation will serve as benchmarks for the software that produced them. Benchmarking is an important, if unexciting, process in all software development.

1.2 Literature Review

There is currently a dearth of publicly available data regarding the burnup of SFRs and its impact on the fuel cycle. However, there is no such shortage of information regarding the economic viability of the SFR and its value as an agent in a transition to Gen-IV reactors.

Ko and Gao found the SFR to be the most cost-competitive reactor model in Korea. The primary advantage of the fast reactor, they write, is that the SFR "can burn both U-235 and transuranic elements (TRUs). This aspect makes it possible to transmute the TRUs and extract energy at the same time." (W. Ko and F. Gao, p3). Ko and Gao do not extensively investigate the impact of SFR deployment on the fuel cycle, instead they focus on its economic viability with regards to front-end loads and Uranium pricing. Park et al investigated the viability of the fuel cycle with an SFR fleet, and found it to be "the most competitive" relative to Once-Through, DUPIC, and PWR MOX, (Park et al, p1).

Some attention has also been given to the optimization of the BOC fuel composition of the SFR. Zhang, Wallenius, and Fuko found through transient analysis simulation with SERPENT that the addition of Americium to the fresh fuel prevents several hazardous accidents and failures. They suggest a weight fraction of 2-3% for Americium in a MOX fuel SFR to optimize safety (Zhang, Wallenius, and Fuko, p1).

1.3 Tabulation of Design Parameters

As mentioned above, the reactor of interest to this investigation is a 1000-MWth metallic-fuel core SFR. The active core of the SFR is 85.82 cm in height, sandwiched between lower and upper reflectors that are 125.15 and 112.39 cm in height (NEA, p27). For simplicity, the axial reflectors were not included in the simulation. The core layout is detailed in figure 1. The average temperature of the coolant and structural materials is 432.5 C, and the average temperature of the fuel is 534 C. In the simulation, these values were approximated to 600 K and 900 K.

The fuel is divided into two regions, the inner and outer core, with different enrichments. Both regions are further divided into five layers with various fuel compositions, given in tables 5 and 6. The layout of the driver subassembly is the same everywhere in the SFR. This layout is given by figure 2 (NEA, p26).

The fuel, shield, control, and reflector subassemblies all have a pitch of 16.2471 cm. Each assembly type has a unique number of pins and pin pitch. Parameters for these assemblies are given in tables 1 through 4 (NEA, p23-24). The isotopic compositions of the materials used in these assemblies are given in tables 7 through 9 (NEA, p29)

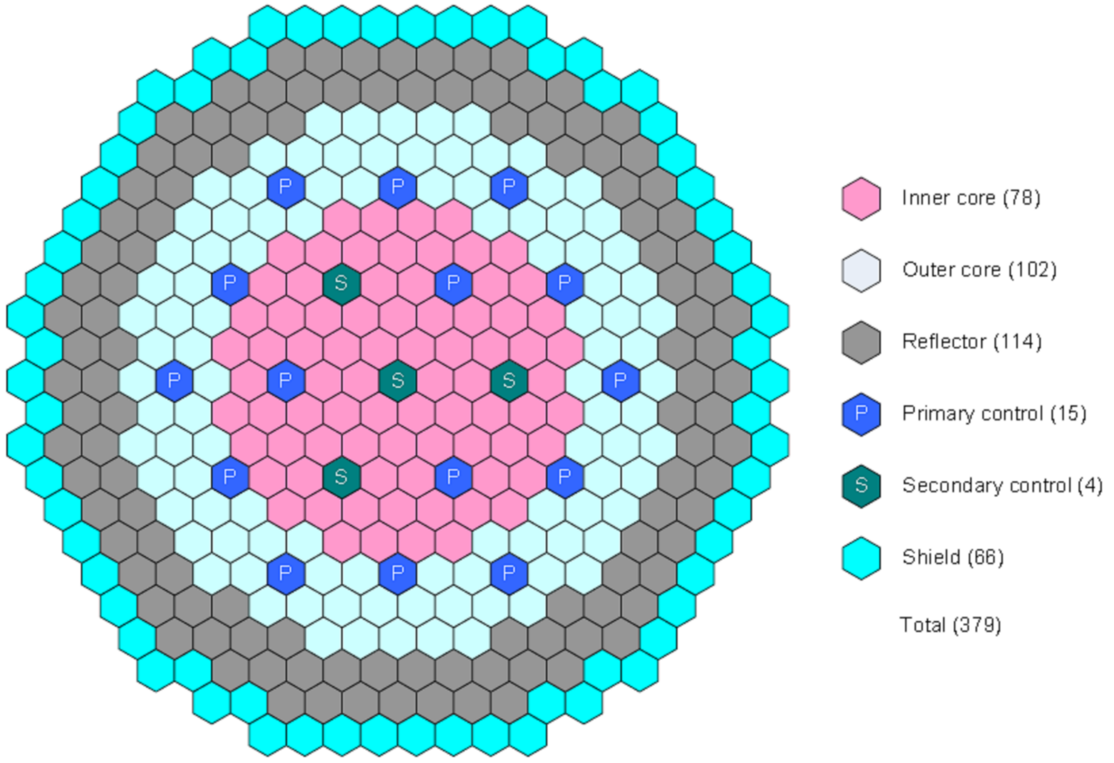

Figure 1. Radial Core Layout of the SFR. There are six different subassembly types, listed in the legend.

Table 1. Fuel Subassembly Parameters

Parameter	Length (cm)
Overall length of subassembly	480.2
Subassembly pitch	16.2471
Subassembly duct outer flat-to-flat distance	15.8123
Subassembly duct wall thickness	0.3966
Outer radius of cladding	0.3857
Inner radius of cladding	0.3236
Fuel slug radius	0.3236
Fuel pin pitch	0.93802
Number of fuel pins: 271	

Table 2. Shield Subassembly Parameters	
Parameter	Length (cm)
Overall length of subassembly	480.2
Subassembly pitch	16.2471
Subassembly duct outer flat-to-flat distance	15.8123
Subassembly duct wall thickness	0.3966
Outer radius of cladding	0.3857
Inner radius of cladding	0.3236
Absorber Radius	0.3236
Fuel pin pitch	3.12674
Number of fuel pins: 19	

Table 3. Control Subassembly Parameters	
Parameter	Length (cm)
Overall length of subassembly	480.2
Subassembly pitch	16.247
Subassembly duct outer flat-to-flat distance	15.812
Subassembly duct wall thickness	0.3966
Outer radius of cladding	2.3606
Inner radius of cladding	2.289
Absorber radius	2.289
Fuel pin pitch	4.6901
Number of fuel pins: 7	

Table 4. Reflector Subassembly Parameters	
Parameter	Length (cm)
Overall length of subassembly	480.2
Subassembly pitch	16.2471
Subassembly duct outer flat-to-flat distance	0.3966
Rod radius	0.7757
Number of fuel pins: 91	

Table 5. Inner core isotopic composition

Nuclide	Upper boundary from active core bottom (cm)/Density (atoms/barn-cm)					
	17.16	34.33	51.49	68.66	85.82	Average
^{234}U	1.1369E-06	1.0856E-06	1.0727E-06	1.1028E-06	1.1759E-06	1.1148E-06
^{235}U	3.0421E-05	2.9338E-05	2.8961E-05	3.0070E-05	3.2571E-05	3.0272E-05
^{236}U	2.4896E-06	2.5117E-06	2.5536E-06	2.3779E-06	2.0226E-06	2.3911E-06
^{238}U	1.9613E-02	1.9474E-02	1.9433E-02	1.9550E-02	1.9801E-02	1.9574E-02
^{237}Np	4.6686E-05	4.6962E-05	4.6782E-05	4.7603E-05	4.8895E-05	4.7386E-05
^{236}Pu	4.9700E-10	5.5883E-10	5.6701E-10	5.5075E-10	4.8775E-10	5.3227E-10
^{238}Pu	1.1695E-04	1.1284E-04	1.1196E-04	1.1370E-04	1.1829E-04	1.1475E-04
^{239}Pu	2.2076E-03	2.1814E-03	2.1754E-03	2.1813E-03	2.2011E-03	2.1894E-03
^{240}Pu	1.3244E-03	1.2955E-03	1.2902E-03	1.2986E-03	1.3248E-03	1.3067E-03
^{241}Pu	1.9375E-04	1.8610E-04	1.8518E-04	1.8537E-04	1.8845E-04	1.8777E-04
^{242}Pu	2.9277E-04	2.8911E-04	2.8818E-04	2.9038E-04	2.9569E-04	2.9123E-04
^{241}Am	1.0791E-04	1.0465E-04	1.0353E-04	1.0686E-04	1.1421E-04	1.0743E-04
^{242m}Am	9.2989E-06	9.0848E-06	9.0224E-06	9.1756E-06	9.4890E-06	9.2141E-06
^{243}Am	1.0017E-04	9.8324E-05	9.7993E-05	9.8630E-05	1.0032E-04	9.9087E-05
^{242}Cm	5.6250E-06	5.8208E-06	5.9476E-06	5.4901E-06	4.5416E-06	5.4850E-06
^{243}Cm	5.4321E-07	5.0246E-07	5.0136E-07	4.8876E-07	4.8480E-07	5.0412E-07
^{244}Cm	6.7240E-05	6.5722E-05	6.5622E-05	6.5349E-05	6.5394E-05	6.5865E-05
^{245}Cm	1.7397E-05	1.6743E-05	1.6663E-05	1.6696E-05	1.7026E-05	1.6905E-05
^{246}Cm	9.2285E-06	9.1426E-06	9.1307E-06	9.1364E-06	9.1805E-06	9.1637E-06
Zr	7.2802E-03	7.2802E-03	7.2802E-03	7.2802E-03	7.2802E-03	7.2802E-03
a Mo	9.29E-04	1.15E-03	1.20E-03	1.06E-03	7.41E-04	1.02E-03

*m indicates an isomer, a indicates a pseudo product

Table 6. Outer core isotopic composition

Nuclide	Upper boundary from active core bottom (cm)/Density (atoms/barn-cm)					
	17.16	34.33	51.49	68.66	85.82	Average
^{234}U	1.6317E-06	1.5766E-06	1.5638E-06	1.5894E-06	1.6552E-06	1.6033E-06
^{235}U	3.0822E-05	2.9870E-05	2.9561E-05	3.0391E-05	3.2250E-05	3.0579E-05
^{236}U	1.7881E-06	1.8534E-06	1.8941E-06	1.7528E-06	1.4710E-06	1.7519E-06
^{238}U	1.8244E-02	1.8144E-02	1.8115E-02	1.8191E-02	1.8359E-02	1.8211E-02
^{237}Np	9.8244E-05	9.7300E-05	9.6775E-05	9.8481E-05	1.0175E-04	9.8510E-05
^{236}Pu	7.1175E-10	8.2505E-10	8.4282E-10	8.0703E-10	6.8053E-10	7.7344E-10
^{238}Pu	1.6436E-04	1.6026E-04	1.5949E-04	1.6063E-04	1.6416E-04	1.6178E-04
^{239}Pu	2.8147E-03	2.7664E-03	2.7538E-03	2.7786E-03	2.8416E-03	2.7910E-03
^{240}Pu	1.7467E-03	1.7191E-03	1.7135E-03	1.7231E-03	1.7508E-03	1.7306E-03
^{241}Pu	2.8976E-04	2.8138E-04	2.8012E-04	2.8135E-04	2.8697E-04	2.8392E-04
^{242}Pu	4.0754E-04	4.0412E-04	4.0321E-04	4.0530E-04	4.1028E-04	4.0609E-04
^{241}Am	1.8607E-04	1.8127E-04	1.7970E-04	1.8397E-04	1.9339E-04	1.8488E-04
^{242m}Am	1.2185E-05	1.2045E-05	1.2021E-05	1.2039E-05	1.2064E-05	1.2071E-05
^{243}Am	1.3234E-04	1.3019E-04	1.2985E-04	1.3036E-04	1.3206E-04	1.3096E-04
^{242}Cm	6.4688E-06	6.8630E-06	7.0553E-06	6.4446E-06	5.1976E-06	6.4059E-06
^{243}Cm	6.3471E-07	6.0893E-07	6.0901E-07	5.9753E-07	5.9372E-07	6.0878E-07
^{244}Cm	8.0107E-05	7.8889E-05	7.8847E-05	7.8479E-05	7.8359E-05	7.8936E-05
^{245}Cm	2.0200E-05	1.9678E-05	1.9613E-05	1.9635E-05	1.9913E-05	1.9808E-05
^{246}Cm	1.0443E-05	1.0371E-05	1.0361E-05	1.0367E-05	1.0410E-05	1.0390E-05
Zr	7.2802E-03	7.2802E-03	7.2802E-03	7.2802E-03	7.2802E-03	7.2802E-03
a)Mo	8.1524E-04	1.0174E-03	1.0697E-03	9.4870E-04	6.6172E-04	9.0255E-04

*m indicates an isomer, a indicates a pseudo product

Table 7. Isotopic Composition of non-Fuel Components

Material	Isotope	Atomic Density (atoms/barn-cm)
Coolant	Na	2.2272E-02
HT-9	Fe	6.9715E-02
	Ni	4.2984E-04
	Cr	1.0366E-02
	^{55}Mn	4.5921E-04
	Mo	4.9007E-04
Natural B_4C	C	1.9657E-02
	^{10}B	1.5018E-02
	^{11}B	6.3609E-02
Enriched B_4C	C	2.0632E-02
	^{10}B	5.3642E-02
	^{11}B	2.8884E-02

2. Methods

This investigation analyzed a 1000-MWth SFR with the Finnish reactor simulator Serpent2. The University of Illinois at Urbana Champaign campus cluster performed the simulations and produced all of the data in this report. All code was produced in a Windows environment, which was also used to communicate with the cluster. These decisions were the source of many delays and bugs during the investigation. Because the cluster is a Linux environment, all plaintext files that were produced in Windows had to be converted from the DOS format to UNIX. Furthermore, the campus cluster is an inefficient environment for debugging, as the investigation had to pause for several hours to wait for the cluster every time the code was updated.

Serpent2 was an excellent choice of software for this investigation. Writing inputs for Serpent is fairly simple, and the Serpent User Guide is thorough and helpful.

2.1 Software and Code

Serpent2 is a Monte Carlo based simulator code that uses a stochastic approach to approximate fuel burnup in a reactor given the geometry and material properties as inputs (Lepannen, p2). Serpent may function as a steady state simulator, an independent burnup calculator, or in a coupled mode (Lepannen, p108). The program creates a unionized energy grid of neutrons, and is resource-intensive as a consequence. Serpent typically requires more than 3 gigabytes of RAM to perform burnup calculations (Lepannen, p2).

The input data are organized into many cards of various types, including pin, lattice, surface, cell, and material. The cross-sections, decay paths, and fission yields of every nuclide in the reactor are accessed via the inclusion of ACE, NFY, and DEC libraries. In this investigation, these libraries were provided by the ARFC research group.

The geometry in Serpent is based on universes of various levels (Lepannen, 12). The simplest level of the geometry is the pin, an annular nest of materials that are defined by the material cards. This investigation used fourteen pin types. Ten pin types describe the ten different fuel compositions, three pin types are required for the reflector, shield, and control assemblies, and a coolant pin was added to the input to serve as an outer boundary of the subassemblies. The typical syntax of the pin card is as follows:

```
pin <u>
<mat> <r1>
clad <r2>
cool
```

In which *<u>* is the universe number assigned to the pin, *<mat>* is the alias of the material inside of the pin, and *<r1>* and *<r2>* are the inner and outer radii of the cladding. The string "clad" calls the cladding material, HT-9 steel. Every pin was assigned a two-digit universe number to more easily manage the spacing in the lattice cards. The coolant, reflector, shielding, and control pins were numbered 10, 13, 14, and 15, respectively. The inner and outer core fuel pins were named <n1> and <n2>, in which n represented the vertical position in the active core, starting with 1 for the bottom layer and ending with 5 for the top layer.

The next level of universes in the geometry are the subassembly lattices. There are thirteen subassemblies, one for each pin type other than the coolant pin. Each subassembly is a y-type hexagon composed of coolant and the main pin. The syntax of the subassembly is as follows (Lepannen, p30):

```
lat <u> 3 0 0 <n> <n> <p>
10 10 10 10 10 10
 10 10 xx xx xx 10
  10 xx xx xx xx 10
   10 xx xx xx 10 10
    10 10 10 10 10 10
```

In which <*u*> is the universe number of the subassembly, *xx* is the universe number of the pin, <*n*> is the number of elements horizontally and vertically (in this investigation, these values were always equal) and p is the pin pitch. The pin pitch is not given explicitly by the benchmark, and was derived with the following equation:

$$p = s/n = P/n\,tan(\pi/6) \; = \; 9.38021/n$$

In which s is the side length of the subassembly and P is the subassembly pitch. The numbering system for these subassemblies is similar to the numbering system used with the pins. Each lattice is given a two-digit universe number. The inner and outer fuel subassemblies are numbered n7 and n8, with n representing the vertical layer of the subassembly, as before. The reflector, shielding, and control subassemblies are numbered 23 through 25.

These subassemblies were then arranged into five different lattices, which model each layer of the core. The syntax of these lattices were as follows:

```
lat n 2 0 0 25 25 16.2471

10 10 10 10 10 10 10 10 10 10 10 10 10 10 10 10 10 10 10 10 10 10 10 10 10
 10 10 10 10 10 10 10 10 10 10 10 10 10 10 24 24 24 24 24 24 24 24 10 10 10
  10 10 10 10 10 10 10 10 10 10 10 10 24 24 23 23 23 23 23 23 23 24 24 10 10
   10 10 10 10 10 10 10 10 10 10 24 24 23 23 23 23 23 23 23 23 23 23 24 24 10
    10 10 10 10 10 10 10 10 10 24 23 23 23 23 n8 n8 n8 n8 n8 23 23 23 23 24 10
     10 10 10 10 10 10 10 10 24 23 23 23 n8 n8 n8 n8 n8 n8 n8 n8 23 23 23 24 10
      10 10 10 10 10 10 10 24 23 23 n8 n8 25 n8 n8 25 n8 n8 25 n8 n8 23 23 24 10
       10 10 10 10 10 10 24 23 23 n8 n8 n8 n8 n7 n7 n7 n7 n8 n8 n8 n8 23 23 24 10
        10 10 10 10 10 24 23 23 n8 n8 n8 n7 n7 n7 n7 n7 n7 n7 n8 n8 n8 23 23 24 10
         10 10 10 10 24 23 23 n8 n8 25 n7 n7 25 n7 n7 25 n7 n7 25 n8 n8 23 23 24 10
          10 10 10 24 23 23 n8 n8 n8 n7 n7 n7 n7 n7 n7 n7 n7 n7 n8 n8 n8 23 23 24 10
           10 10 10 24 23 23 n8 n8 n7 n7 n7 n7 n7 n7 n7 n7 n7 n7 n8 n8 23 23 24 10 10
            10 10 24 23 23 n8 25 n8 n7 25 n7 n7 25 n7 n7 25 n7 n8 25 n8 23 23 24 10 10
             10 10 24 23 23 n8 n8 n7 n7 n7 n7 n7 n7 n7 n7 n7 n7 n8 n8 23 23 24 10 10 10
              10 24 23 23 n8 n8 n8 n7 n7 n7 n7 n7 n7 n7 n7 n7 n8 n8 n8 23 23 24 10 10 10
               10 24 23 23 n8 n8 25 n7 n7 25 n7 n7 25 n7 n7 25 n8 n8 23 23 24 10 10 10 10
                10 24 23 23 n8 n8 n8 n7 n7 n7 n7 n7 n7 n7 n8 n8 n8 23 23 24 10 10 10 10 10
                 10 24 23 23 n8 n8 n8 n8 n7 n7 n7 n7 n8 n8 n8 n8 23 23 24 10 10 10 10 10 10
                  10 24 23 23 n8 n8 25 n8 n8 25 n8 n8 25 n8 n8 23 23 24 10 10 10 10 10 10 10
                   10 24 23 23 23 n8 n8 n8 n8 n8 n8 n8 n8 23 23 23 24 10 10 10 10 10 10 10 10
                    10 24 23 23 23 23 n8 n8 n8 n8 n8 23 23 23 23 24 10 10 10 10 10 10 10 10 10
                     10 24 24 23 23 23 23 23 23 23 23 23 23 24 24 10 10 10 10 10 10 10 10 10 10
                      10 10 24 24 23 23 23 23 23 23 23 24 24 10 10 10 10 10 10 10 10 10 10 10 10
                       10 10 10 24 24 24 24 24 24 24 24 10 10 10 10 10 10 10 10 10 10 10 10 10 10
                        10 10 10 10 10 10 10 10 10 10 10 10 10 10 10 10 10 10 10 10 10 10 10 10 10
```

In this snippet, n is the layer number of the lattice. This is a type 2-lattice, which corresponds to the x-type hexagon. In reality, the core is octagonal in shape, but using the hexagonal shape provides a good enough approximation.

Only three more cards are needed to complete the geometry. The next card is a type 9 lattice to stack the assemblies (Lepannen, p31):

```
lat 6 9 0 0 5
0.0   1
17.16 2
34.33 3
51.49 4
68.66 5
```

This card gives the value of the upper boundary of each layer in the boundary. These values are taken from tables 5 and 6. Then, a surface card to bind the universes (Lepannen, p21):

```
surf 1 hexyprism .0 .0 165.0  0.0 85.82
```

Again, a hexagon is used to approximate the octagonal shape of the reactor. Here, 165.0 sets the distance between the core's center and its vertical edge. Finally, two cells are placed on either side of the boundary surface with the following code (Lepannen, p24):

```
cell 1  0 fill 6  -1 %1000 -1001
cell 99 0 outside  1 %outside world
```

Figures 2 through 4 are the output when the geometry plotter is applied to the code as described above. Figure 2 closely resembles Figure 1, the core schematic, indicating that the geometry was built correctly.

However, completing the geometry is not the final goal of this investigation. In order to complete burnup calculations, Serpent needs more information about the reactor. Specifically, 14 material cards (ten for the fuel, and one each for the HT9 steel, coolant, and the enriched and natural Boron Carbide are required. These material cards are simple, and use the following syntax:

```
mat <alias> sum burn 1
<ZAID1> <dens1>
<ZAID2> <dens2>
...
<ZAIDn> <densn>
```

In which <alias> is the name of the material, <ZAID> is the ID of the nuclide (1000*Z + A), <dens> is the atomic density in atoms/barn-cm, "sum" tells the program that the density of the material can be calculated from the sum of the constituent parts, and "burn 1" signals that the material is a part of burnup calculations. "Burn 1" should only be included in the material cards that define the fuel (Lepannen, p47).

3. Results

The preceding code will run in SERPENT2 without any bugs or errors. The total computation required almost 6 hours of CPU time on the UIUC campus cluster, and ran in approximately 20 minutes of wall-time. There were approximately 34 MB of output files, all of which are stored in the aforementioned GitHub repository. Included in these outputs are text files listing the isotopic composition of the depleted fuel and several images of the reactor core. Two of the geometry plots (which use various colors to plot the locations of materials in the reactor) and four of the mesh plots (which use bright and dark colors to plot the locations of relatively high and low activities in the reactor) are displayed in figures 2 through 7.

The criticality value for the reactor is approximately 0.8, largely due to the fact that it was simulated with its control rods fully inserted. This simplification is the cause of some uncertainty in the results of this investigation, but probably did not result in any significant changes in the results.

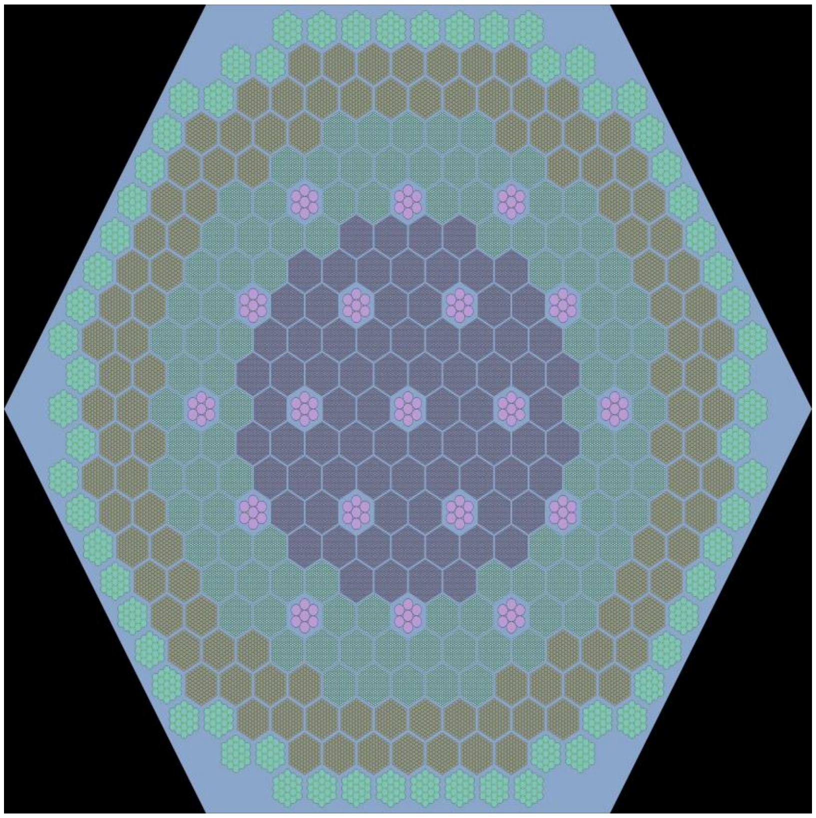
Figure 2. The first geometry plot of the SFR. The view is from above the reactor

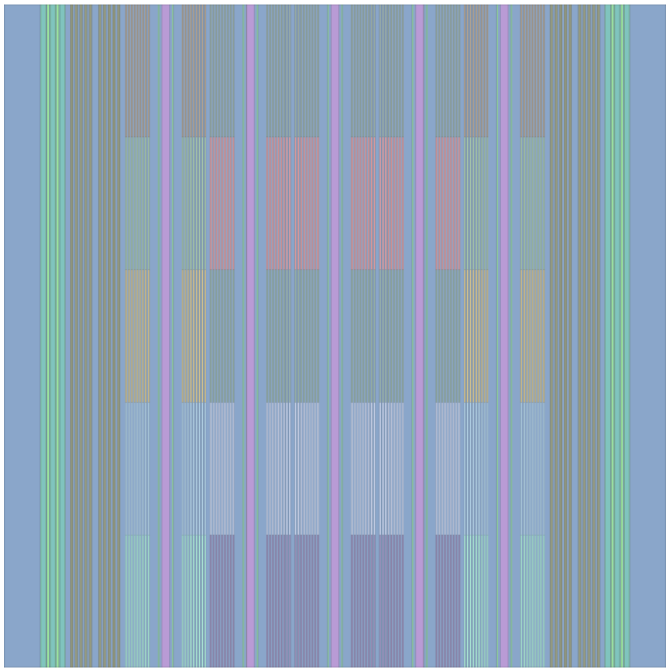
Figure 3. The second geometry plot of the SFR. The view is parallel to the x axis, it shows the reactor from the side. Note the 5 layers of fuel and fully inserted control rods.

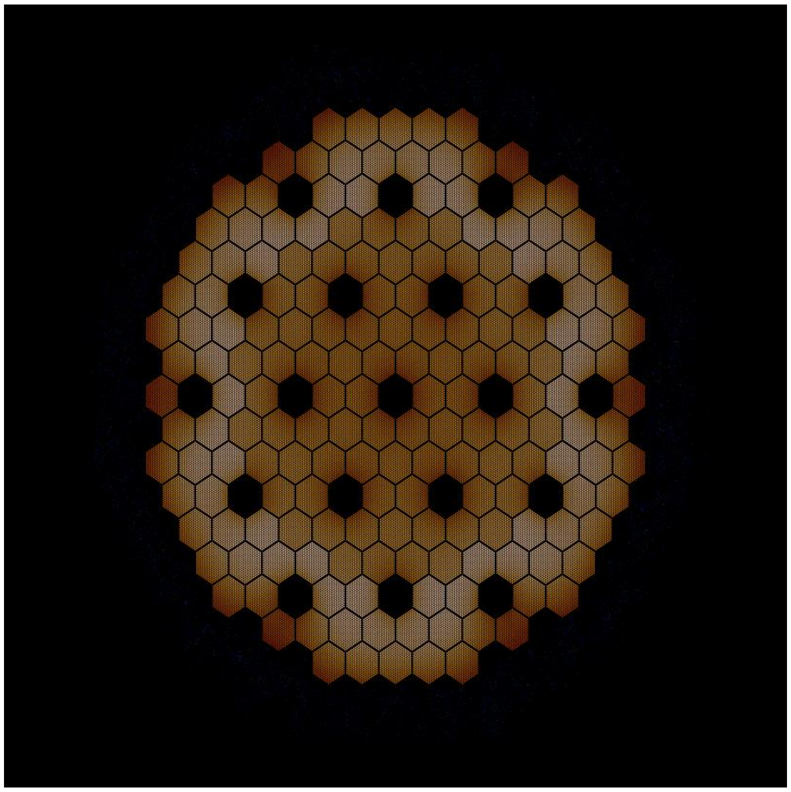

Figure 4. The first BOC mesh plot. This view is from above the reactor. Darker hues of orange indicate greater activity. Black regions are inactive.

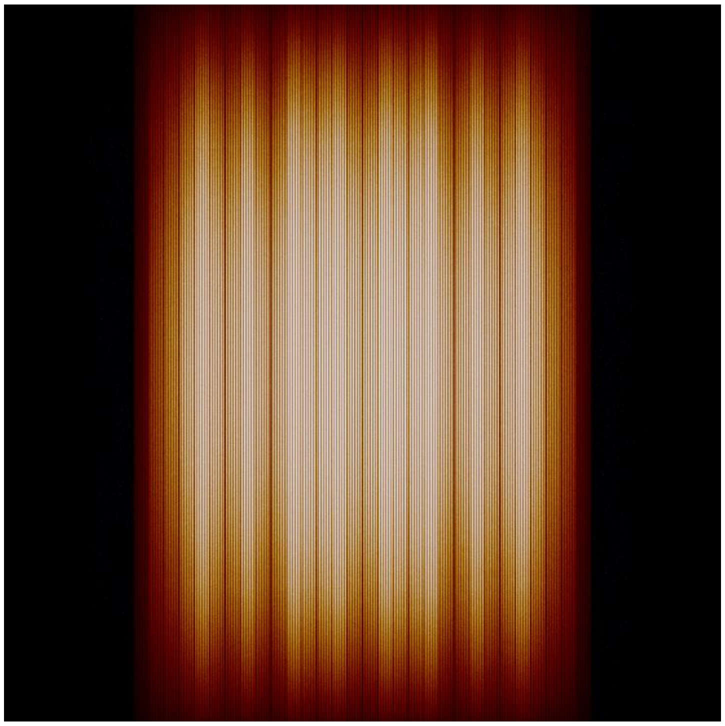

Figure 5. The second BOC mesh plot. This view is from the side of the reactor.

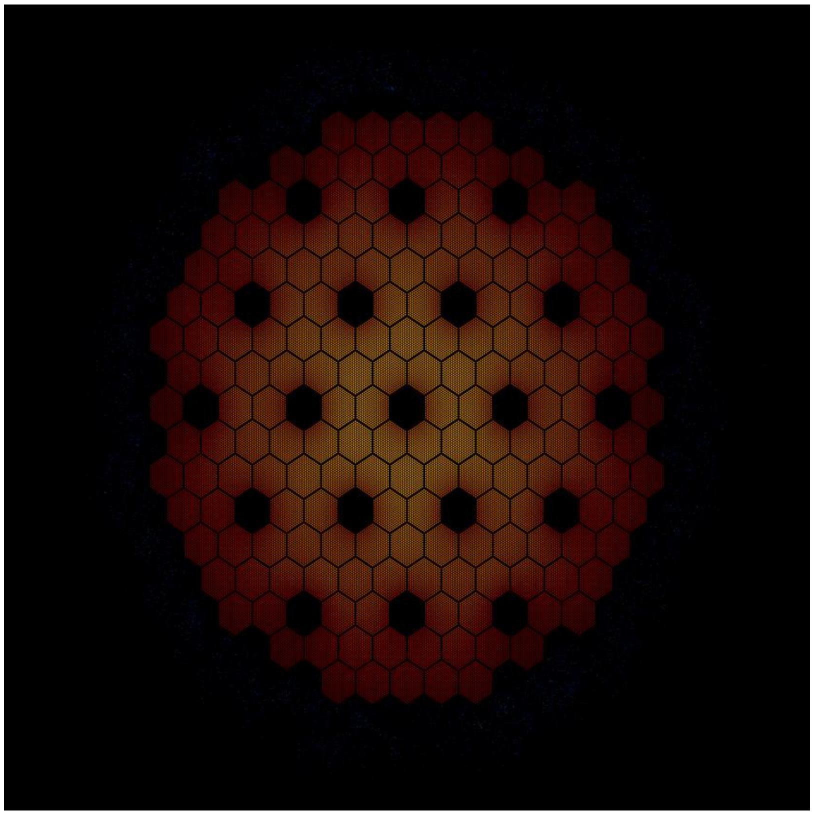
Figure 6. The first EOC mesh plot. The mesh is overall dimmer than its BOC counterpart, indicating that the fuel is depleted.

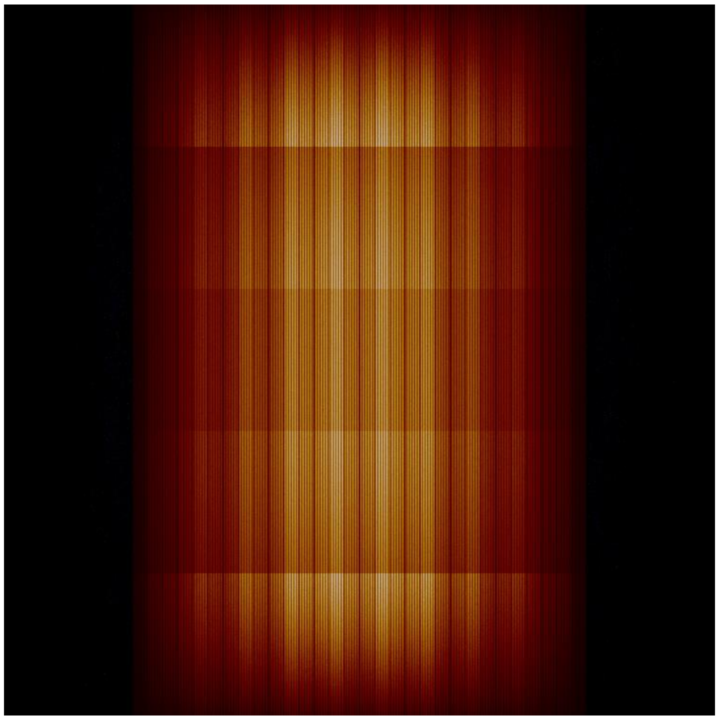
Figure 7. The second EOC mesh plot. This view is from the side of the reactor.

4. Conclusions

This investigation simulated one year of operation of a 1000-MWth sodium-cooled fast reactor with a metal-fueled core using the SERPENT2 Monte Carlo reactor simulator. The results of this investigation will be shared with the UIUC ARFC research group, who will use the data to perform fuel cycle analysis and evaluate the viability of transition scenarios.

During the course of this investigation, several noteworthy assumptions were made that in all likelihood cause insignificant changes to the results and output data of the investigation. Regardless, they deserve explication here. All axial reflectors and structures were ignored in the simulation. Because of this, more neutrons were lost out of the top and bottom of the reactor, which probably reduced its criticality. All control rods were fully deployed for the entire operation time of the reactor. This significantly reduced the criticality of the reactor. Finally, the reactor was designed as a regular hexagonal object, when it is actually an irregular octagon.

The input code that was developed for this investigation should be relatively easy to modify to simulate the burnup of other SFRs with different power, fuel compositions and fuel types. With further effort, code could be produced to simulate other advanced reactors to facilitate further analysis of transition scenarios and fuel cycles regarding those reactor types.

If the investigations discussed above were to proceed, they would do well to learn from the mistakes of this investigation. First, Windows should be abandoned as a computing environment in favor of GNU/Linux. Windows did nothing but hinder this investigation by producing bugs and requiring the installation of special SSH programs. Additionally, the debugging process took much longer than necessary because SERPENT2 was only used remotely. The use of the campus cluster was helpful for handling the larger computations, but led to several-hour wait times, which probably increased the debugging time tenfold.

References

1) NEA (February 2016). *Benchmark for Neutronic Analysis of Sodium-cooled Fast Reactor Cores with Various Fuel Types and Core Sizes*, Retrieved from www.oecd-nea.org
2) J. Leppänen (June 18, 2015), *Serpent – a Continuous-energy Monte Carlo Reactor Physics Burnup Calculation Code*. VTT Technical Research Centre of Finland. Retrieved From: http://montecarlo.vtt.fi
3) Ko, W., Gao, F, (February 2, 2012). *Economic Analysis of Different Nuclear Fuel Cycle Options*, Korea Atomic Energy Research Institute, Yuseong, Daejeon 305-353, Republic of Korea, Retrieved From: https://www.hindawi.com/journals/stni/2012/293467/
4) Park, B., Gao, F., Kwon, E., Ko, W., (November, 2011). *Comparative study of different nuclear fuel cycle options: Quantitative analysis on material flow,* Retrieved From: http://www.sciencedirect.com/science/article/pii/S0301421511002801
5) Zhang, Y., Wallenius, J., Fokau, A., (May, 2010). *Transmutation of americium in a medium size sodium cooled fast reactor design*, Retrieved From: http://www.sciencedirect.com/science/article/pii/S0306454909003880